

NOTICE: This is the author's version of a work that was accepted for publication in *Food Hydrocolloids*. Changes resulting from the publishing process, such as peer review, editing, corrections, structural formatting, and other quality control mechanisms may not be reflected in this document. Changes may have been made to this work since it was submitted for publication. A definitive version was subsequently published in *Food Hydrocolloids*, 2016,61,504-513. doi <https://doi.org/10.1016/j.foodhyd.2016.05.029>

This item is made available to you under the Creative Commons Attribution-Non commercial-No Derivatives 3.0 License.



Covalent labelling of  $\beta$ -casein and its effect on the microstructure and physico-chemical properties of emulsions stabilised by  $\beta$ -casein and whey protein isolate

Meng Li<sup>1,2</sup>, Mark A.E. Auty<sup>1</sup>, James A. O'Mahony<sup>2</sup>, Alan L. Kelly<sup>2</sup>, André Brodkorb<sup>1\*</sup>

<sup>1</sup>*Teagasc Food Research Centre, Moorepark, Fermoy, Co. Cork, Ireland*

<sup>2</sup>*School of Food and Nutritional Sciences, University College Cork, Cork, Ireland*

\*Corresponding author.

Tel.: +353 25 42431

E-mail address: [andre.brodkorb@teagasc.ie](mailto:andre.brodkorb@teagasc.ie)

## Abstract

The objective of this work was to investigate the effect of covalent labelling on the physico-chemical properties of  $\beta$ -casein ( $\beta$ -CN) in solution and in emulsions stabilised by  $\beta$ -CN and whey protein isolate (WPI).  $\beta$ -CN was covalently labelled by 5-(and 6)-carboxytetramethylrhodamine, succinimidyl ester (NHS-Rhodamine). The effect of conjugating  $\beta$ -CN with NHS-Rhodamine on the spectroscopic properties of labelled  $\beta$ -CN ( $\beta$ -CN<sub>labelled</sub>) was examined. No significant difference in interfacial tension ( $p>0.05$ ) was found between mixture of WPI and  $\beta$ -CN<sub>labelled</sub> (0.5% w/w WPI/ $\beta$ -CN<sub>labelled</sub>) and of WPI and  $\beta$ -CN (0.5% w/w WPI/ $\beta$ -CN) in 10 mM phosphate buffer (pH 7.0) at 20 °C. Oil-in-water emulsions stabilized with either WPI/ $\beta$ -CN or WPI/ $\beta$ -CN<sub>labelled</sub> (0.5% w/w) were also investigated using laser-light scattering, analytical centrifugation, rheometry and CLSM. It was shown that labelling had no significant effect on the physico-chemical properties of emulsions ( $p>0.05$ ) in terms of droplet size, creaming stability, viscosity or zeta-potential. Confocal micrographs of emulsions made with WPI/ $\beta$ -CN<sub>labelled</sub> showed that both  $\beta$ -CN and whey proteins could be observed simultaneously, and were co-localized at the surface of fat globules. Furthermore, it was found through image analysis that  $\beta$ -CN produced a thicker interfacial layer than WPI.

**Keywords:**  $\beta$ -casein, whey proteins, emulsion stability, confocal laser scanning microscopy, covalent labelling techniques

## 1. Introduction

Dairy proteins are often used as emulsifiers in a variety of dairy products. They adsorb at the surface of newly formed oil droplets during homogenization, thereby producing a layer to protect the oil droplets against coalescence and flocculation during storage. The nature of the adsorbed layer at the oil-water interface is one of the most important factors determining the physico-chemical behaviours of emulsions, and a large number of studies have explained the adsorption behaviours of proteins on the oil droplets surface (Dickinson, 2001; Dickinson & Parkinson, 2004; McClements, 2004; McSweeney, Mulvihill, & O'Callaghan, 2004; Raikos, 2010).

Dairy proteins are classified into two main categories: caseins and whey proteins. Caseins consisting of  $\alpha_{s1}$ -,  $\alpha_{s2}$ -,  $\beta$ - and  $\kappa$ -casein are self-assembled in milk into particles called casein micelles with  $\kappa$ -casein located predominately at the surface of the micelle (Fox & McSweeney, 2003). Caseins are relatively heat-stable but tend to aggregate upon lowering the pH and become insoluble at their isoelectric point of pH 4.6 (Hammarsten, 1883; L., Slyke, & Barker, 1918). All caseins have a large proportion (35-45%) of hydrophobic amino acid residues (e.g. Val, Leu, Phe, Tyr, Pro), especially  $\beta$ -CN. One of the most abundant caseins,  $\beta$ -CN has a flexible linear disordered secondary structure and no intramolecular crosslinks. It has a hydrophilic region at the N-terminal and a hydrophobic region of zero net charge at the C-terminal of the molecule (Parkinson & Dickinson, 2004; Rollema, 1992).  $\beta$ -CN includes 5 phospho-serines in the hydrophilic part, which gives a high net negative charge (Dickinson, 1997). The presence of phospho-serine residues in  $\beta$ -CN provides the thickness and steric-stabilizing properties of the adsorbed layer surrounding the oil droplets. Its highly amphiphilic nature contributes to the emulsifying properties.  $\beta$ -CN is assumed to be one of the most surface-active dairy proteins (Mitchell, Irons, & Palmer, 1970). It has been reported that  $\beta$ -CN adsorbed more rapidly at the oil-water interfaces and was more effective in reducing the interfacial tension compared with other caseins (Dickinson, 1989). Therefore,  $\beta$ -CN is widely used as an effective emulsifier in formulated emulsion systems. In addition,  $\beta$ -casein exists in solution in a molecular or aggregated state depending on the concentration, temperature and ionic strength. It was concluded (Dauphas, et al., 2005) that at low temperature ( $< 15\text{ }^{\circ}\text{C}$ ),  $\beta$ -casein generally is found as monomers with a mean diameter of 7-8 nm. It aggregates into a micellar state with a diameter of 20-25 nm when temperature increases to  $35\text{ }^{\circ}\text{C}$  in the absence of salt. Adding calcium ( $\text{Ca}^{2+}$ ) leads to formation

of  $\beta$ -CN sub-micelles or aggregates because the electrostatic repulsion between molecules decreases when calcium associates with phosphoserine residues. McCarthy, Kelly, O'Mahony, and Fenelon (2013) illustrated that calcium-induced aggregation was decreased when dephosphorylated bovine  $\beta$ -CN was used to stabilize emulsions.

The major whey proteins in bovine milk are  $\beta$ -lactoglobulin ( $\beta$ -lg),  $\alpha$ -lactalbumin ( $\alpha$ -la) and bovine serum albumin (BSA). They are compact globular proteins characterised by well-defined three-dimensional structures held together by di-sulphide bonds. Whey proteins are sensitive to temperature and are readily denatured at temperature  $> 75$  °C (Millqvist-Fureby, Elofsson, & Bergenståhl, 2001). Many studies have shown that caseins (e.g.  $\alpha_{s1}$ -,  $\alpha_{s2}$ -,  $\beta$ - and  $\kappa$ -casein) can act in a similar manner as molecular chaperones to inhibit the thermal denaturation of whey proteins (Guyomarc'h, Nono, Nicolai, & Durand, 2009; Kehoe & Foegeding, 2011, 2014; Morgan, Treweek, Lindner, Price, & Carver, 2005; O'Kennedy, Mounsey, Murphy, Duggan, & Kelly, 2006). Whey proteins are used as dairy ingredients due to their nutritional and functional properties. They are also excellent emulsifiers, and are slightly less surface active than caseins (Hunt & Dalgleish, 1994). Previous studies have shown that the inhibition of droplet flocculation can be achieved in whey protein-stabilized emulsions by incorporation of very small amounts (e.g. 0.015% w/w  $\beta$ -CN in the total emulsion) of casein (Dickinson & Parkinson, 2004; Parkinson & Dickinson, 2004). Whey protein isolate (WPI) is a commercially available whey protein product, which is produced by either selective ion exchange technology (e.g. BiPRO<sup>®</sup>) or a membrane-based separation process. It contains a higher protein content (90-95% on a dry weight basis) compared to cheaper whey protein concentrate (WPC, generally 30-70% protein) and (sweet/acid) whey powder (9-13% protein).

Microscopy techniques are widely applied for visualising and interpreting physical and chemical analyses. Confocal laser scanning microscopy (CLSM) has been used to visualise different food structures, such as cheese, mayonnaise, milk powder and meat (Auty, Twomey, Guinee, & Mulvihill, 2001; Maher, Auty, Roos, Zychowski, & Fenelon, 2015). Emulsion fat droplet size can be observed directly using CLSM for comparison with the results from light scattering (Lopez, Madec, & Jimenez-Flores, 2010). van de Velde, Weinbreck, Edelman, van der Linden, and Tromp (2003) described how improved contrast may be obtained by differences in fluorescence, either by auto-fluorescence of the material or by the addition of fluorescent dyes. It is possible to stain proteins, fats and polysaccharides

simultaneously using various fluorescent probes/dyes *via* covalent or non-covalent labelling (Auty, 2013; Dickinson & Yamamoto, 1996). Single or multiple probes have been frequently used to observe the phase distribution of protein/fat system and protein/polysaccharide system (Abhyankar, Mulvihill, Chaurin, & Auty, 2011; Ciron, Gee, Kelly, & Auty, 2010). For example, the visualization of fats and proteins in food could be achieved using either Nile blue only (Brooker, 1995) or a mixture of Nile Red and Fast Green FCF (Auty, et al., 2001). Covalent labelling of polymers allows for an exact measurement of multiple components in a system without over-staining. Covalently-labelled proteins can be used to visualize one specific protein in a complex system. There are a variety of reactive commercial protein probes with different fluorescence properties, such as carboxylic acid succinimidyl ester, isothiocyanate or sulphonyl halides. They bind to the reactive amine groups of the proteins *via* covalent bonds under slightly alkaline conditions (van de Velde, et al., 2003).

However, it is difficult to determine if the physico-chemical properties of the labelled protein have changed compared to those of the native form due to the labelling process. For most situations, it is assumed that labelling does not change the properties of the labelled component, without verifying the effect of the labelling on the physical characteristics of modified component.

The main objectives of this study were: (1) to investigate the effect of conjugating  $\beta$ -CN with NHS-Rhodamine, using the covalent labelling technique, on the physico-chemical properties of labelled  $\beta$ -CN ( $\beta$ -CN<sub>labelled</sub>); (2) to examine whether covalent labelling with NHS-Rhodamine can be used to distinguish whey proteins from  $\beta$ -CN in emulsions, using CLSM; and (3) to determine the effect of covalent labelling of  $\beta$ -CN on the physico-chemical properties of emulsions stabilized with WPI/ $\beta$ -CN at neutral pH and room temperature.

## 2. Materials and methods

### 2.1 Materials

Whey protein isolate (WPI, BiPRO<sup>®</sup>) was obtained from Davisco Foods International Inc. (Le Sueur, Minnesota, USA). The protein content (93.3%) was determined in-house by the Kjeldahl method (IDF Standard, 26, 2001) using a nitrogen-to-protein conversion factor of 6.38.  $\beta$ -casein, from bovine milk ( $\geq$  98 % purity) and phosphate buffered saline, pH 7.4 (containing 0.47% phosphate buffer, 0.1% KCl and 4% NaCl, w/v) were purchased from Sigma-Aldrich (St. Louis, MO, USA). Commercial sunflower oil was obtained from Tesco Supermarkets Ltd (Co. Cork, Ireland) and used without purification. NHS-Rhodamine was supplied by Thermo Fisher Scientific (Rockford, IL, USA). Unless otherwise specified, all other reagents were purchased from Sigma Chemicals Inc. (St. Louis, Missouri, USA).

### 2.2 Conjugation of $\beta$ -CN with NHS-Rhodamine *via* covalent labelling techniques

The covalent labelling technique is designed to visualize one specific protein in a complex mixture and to overcome the uncertainties that arise from the use of free fluorescent dyes. In this study,  $\beta$ -CN was covalently labelled using NHS-Rhodamine which reacts specifically with primary amine groups including the amino terminus of proteins and the  $\epsilon$ -amino group of lysine to produce a highly fluorescent conjugate.  $\beta$ -CN was dissolved in 10 mM phosphate buffered saline (10 mg/ml, pH 7.4) before labelling with NHS-Rhodamine (10 mg/ml in DMF, molar ratio of dye:protein = 5:1). The mixture was incubated at room temperature in the dark for 1 h. To remove the unbound dye, the mixture was crudely purified by passing through PD-10 desalting columns (GE Healthcare Life Sciences, Buckinghamshire, UK) under gravity, and then dialysed four times against phosphate buffered saline (10 mM) and twice against distilled water in order to remove the free dye and salt completely (no colour observed). The covalently labelled  $\beta$ -CN solution was then freeze-dried and stored in a desiccator under anhydrous conditions in the dark. The protein concentration % (w/w) and degree of labelling (DOL) of  $\beta$ -CN<sub>labelled</sub> were estimated using Equation (1) and (2), respectively.

$$\text{Protein concentration \% (w/w)} = \frac{\text{weight of labelled protein} - \text{dye concentration} \times \text{volume of labelled protein}}{\text{weight of labelled protein}}$$

(1)

$$\text{Degree of labelling (moles dye per mole protein)} = \frac{\frac{\text{dye concentration (mg/ml)}}{\text{Mw of dye}}}{\frac{\text{protein concentration (mg/ml)}}{\text{Mw of protein}}} \quad (2)$$

Where,

$$\text{Dye concentration (mg/ml)} = \frac{\text{concentration of free dye} \times A_{353} \text{ of labelled protein}}{A_{353} \text{ of free dye}} \times \text{dilution factor}$$

$M_w$  of dye = 528 Da

$M_w$  of protein = 24,000 Da

### 2.3 Determination of native protein concentration by reversed-phase high performance liquid chromatography (RP-HPLC)

The concentration of individual native proteins in WPI was analysed by RP-HPLC (Waters, Milford, MA, USA). Separation was performed on a Source 5RPC column at 28 °C (Amersham Biosciences, UK, Ltd.). The HPLC system consisted of a Waters 2690 Separation Module, a Waters 2487 Dual Lambda Absorbance Detector and Empower Millennium software. Buffer A contained 0.1% (v/v) TFA in Milli-Q® water and buffer B contained 90% acetonitrile and 0.1% TFA in Milli-Q® water. The results indicated that WPI (BiPRO®) contains 19.4 %  $\alpha$ -la, 78.9 %  $\beta$ -lg and 1.7% BSA (native protein).

### 2.4 Spectrophotometric measurements

Solutions of NHS-Rhodamine (5  $\mu$ g/ml),  $\beta$ -CN (0.02%) or  $\beta$ -CN<sub>labelled</sub> conjugate (120  $\mu$ g/ml) were prepared in 10 mM phosphate buffered saline, pH 7.4. The UV/visible absorbance spectra of the solutions were recorded individually in the wavelength range of 250-650 nm, using a Cary 1 Spectrophotometer (Varian Inc., Palo Alto, California, USA).

A Cary Eclipse fluorescence spectrofluorimeter and a 1 cm  $\times$  1 cm quartz cuvette were used to carry out the excitation/emission measurements for NHS-Rhodamine (5  $\mu$ g/ml) and the  $\beta$ -CN<sub>labelled</sub> conjugate solution (120  $\mu$ g/ml) at 25 °C. The instrument settings were as follows: for excitation spectra (450-590 nm)

at a fixed emission wavelength of 600 nm; for emission spectra (530-700 nm) at a fixed excitation wavelength of 525 nm; both excitation and emission slit were 5 nm; scan rate, 600 nm/min.

## 2.5 SDS-Polyacrylamide gel electrophoresis (SDS-PAGE)

$\beta$ -CN<sub>labelled</sub> and native  $\beta$ -CN were characterised by SDS-PAGE in order to study the effect of labelling on  $\beta$ -CN. The procedure was based on that of Laemmli (1970). Briefly, protein samples were dissolved in sample buffer (62.5 mM Tris-HCl buffer, pH 6.8, containing 20% glycerol, 2% (w/v) SDS and 0.025% (w/v) bromophenol blue) to achieve a final concentration of 1  $\mu$ g/ $\mu$ l. For SDS-PAGE under reducing conditions, 5%  $\beta$ -mercaptoethanol was added to samples followed by heating at 95 °C for 5 min. After cooling to room temperature, 5  $\mu$ l of samples were loaded onto a 12% polyacrylamide Amersham ECL gel and run using a Amersham ECL Gel box (GE Healthcare, Uppsala, Sweden). After electrophoresis, the gels were stained for 1 h using 0.05% (w/v) Coomassie brilliant blue R-250 in 25% (v/v) isopropanol and 10% (v/v) acetic acid. After staining, the gels were destained in a 10% (v/v) isopropanol and 10% (v/v) acetic acid solution until a clear background was achieved. Molecular weights ( $M_w$ ) were determined by comparison to pre-stained protein molecular weight markers (Thermo Scientific, MA, USA).

## 2.6 Emulsion preparation

Oil-in-water (O/W) emulsions (10% w/w sunflower oil, 10 mM sodium phosphate buffer, pH 7.0), stabilized with either  $\beta$ -CN or WPI at different concentrations (0.3, 0.4 and 0.5% w/w protein), were pre-mixed using an ultra-turrax<sup>®</sup> model T25 digital (IKA, Staufen, Germany) equipped with a S18N-19G dispersion unit at 6,600 rpm for 15 s. The coarse emulsions were then passed once through a laboratory homogenizer (high pressure laboratory homogenizer, Delta Instruments B.V., Kelvinlaan, Drachten, The Netherlands) at an input pressure of ~ 40 bar. A 0.5% total protein concentration was selected to produce mixed layer emulsions stabilized with WPI and  $\beta$ -CN<sub>labelled</sub> in a protein ratio of 50/50 (w/w). An emulsion made with WPI and  $\beta$ -CN was used as a control. Sodium azide (0.02% w/v) was added as an antimicrobial agent. After homogenization, the pH of all samples was adjusted to 7.0 using HCl or NaOH

and samples were stored at 4 °C cold room. Analyses were carried out at 0 (fresh emulsion) and 3 d post emulsion preparation.

### 2.7 Determination of oil droplet size

The average oil droplet size distribution of each emulsion was determined using a laser-light diffraction unit (Mastersizer 3000, Malvern Instruments Ltd, Worcestershire, UK). The optical parameters chosen were a particle and dispersant refractive index of 1.456 and 1.33, respectively. The absorbance value of the emulsion droplets was 0.01. Laser obscuration was controlled between 5 and 12%. The size distribution was obtained using polydisperse analysis, while droplet size measurements of emulsions were recorded as the sauter mean diameter ( $D_{3,2} = \frac{\sum n_i d_i^3}{\sum n_i d_i^2}$ , where  $n_i$  is the number of droplets with diameter  $d_i$ ) and the volume weighed mean ( $D_{4,3}$ ). Measurements were carried out in triplicate.

### 2.8 Emulsion stability

The stability of emulsions was determined using a multiple analytical centrifuge (LUMiFuge 116 stability analyser, L.U.M GmbH, Berlin, Germany). Aliquots (0.4 ml) were placed in polycarbonate sample cells (2 mm × 8 mm) and centrifuged at 1,500 rpm for 1 h at 25 °C, with transmission profiles measured at 1 min intervals. The result was expressed as the integrated transmission percentage against time. The slope determines the creaming stability of emulsions, with lower values indicating better creaming stability.

### 2.9 $\xi$ -potential measurement

Zeta potential of the emulsions was measured using a Zetasizer Nano-ZS90 (Malvern Instruments, Worcestershire, UK). Emulsions were diluted a 1,000 times using 10 mM sodium phosphate buffer (pH 7) to minimize multiple scattering effects.

### 2.10 Apparent viscosity

Measurement of apparent viscosity was performed using a controlled-stress rheometer (AR2000ex Rheometer, TA Instrument, Crawley, UK), equipped with a concentric cylinder geometry (stator inner radius = 15 mm, rotor outer radius = 14 mm). Each sample (~15 g) was placed into the cylinder,

equilibrated for 2 min before measurement. In order to minimize the effect of water evaporation, a thin layer of n-tetradecane was added to the surface of the sample. The measurement was accomplished over a shear rate range of 10-300 s<sup>-1</sup> at 25 °C.

#### 2.11 Measurement of interfacial tension (IFT)

Measurements of dynamic interfacial tension were carried out as described by Drapala, Auty, Mulvihill, and O'Mahony (2015) with a Krüss K12 Tensiometer at 20 ± 0.5°C over 60 min. Heavy phase (25 ml of 10 mM phosphate buffer or 0.5% protein solutions) and light phase (25 ml of sunflower oil) were used. Interfacial tension was recorded continuously from 0 to 5 min and at 10, 15, 30 and 60 min after forming the interface. The program was set to record a maximum of 80 readings per given time point at 1 sec intervals, unless the standard deviation was ≤ 0.01 in ten consecutive readings, in which case the measurement would stop for the given time point.

#### 2.12 Confocal laser scanning microscopy

Microstructural analysis was performed using a Leica TCS SP5<sup>®</sup> microscope (Leica Microsystems GmbH, Wetzlar, Germany). In order to reducing Brownian motion of particles, low melting point agarose was prepared at 1% (w/v) in distilled water and stored at 45 °C until utilization. Nile blue (100 µl of 0.05% in distilled water) was added to 1 ml of emulsion and mixed thoroughly. Before microstructural observation, sample solutions containing Nile blue were mixed with the agarose in a ratio of 1:3 to immobilise the sample and then 5 µl of each mixture was deposited on a microscope slide. The slide was covered with a coverslip and observed under the microscope at room temperature. The analysis was operated using a 63 × oil immersion objective (numerical aperture 1.4) at excitation wavelengths of 488 (emission detected between 520 and 567 nm) to detect fat, 561 (emission detected between 573 and 613 nm) to detect covalently labelled β-CN and 633 nm (emission detected between 650 and 718 nm) to observe WPI provided by Argon, DPSS and He/Ne lasers, respectively. Images (8 bit) were acquired in 1024 × 1024 pixels using triple channel imaging. The microscope settings were maintained at a similar value for different time point measurements for comparison.

### 2.13 Statistical analysis

The preparation of solutions, emulsions and subsequent analysis were carried out in independent triplicate. Analysis of variance (ANOVA) was carried out using the Minitab 16 (Minitab Ltd, Coventry, UK, 2007) statistical analysis package. The effect of treatment and replicates were estimated. One-way multiple-comparison test was used as a guide for pair comparisons of the treatment means. The level of significance was determined at  $p < 0.05$ .

## 3. Results and discussions

### 3.1 Effect of covalent conjugation of $\beta$ -CN with NHS-Rhodamine on spectroscopic properties

The UV/vis spectra (Fig. 1) showed that 0.05%  $\beta$ -CN solution did not absorb light at any wavelength in the range 350-650 nm. However, it had the expected aromatic absorbance peak at 280 nm. The absorbance spectrum of the NHS-Rhodamine solution (Fig. 1) displayed an absorbance peak at 554 nm. Covalent conjugation of  $\beta$ -CN with NHS-Rhodamine led to a splitting of the main peak into two absorption peaks at about 520 nm and 556 nm (Fig. 1), which may be explained by a non-fluorescent dye aggregation (Haugland, 2005). As most of the free dye was removed by dialysis, aggregation may only occur between dye molecules covalently bound to the protein. The protein concentration and degree of labelling of the  $\beta$ -CN<sub>labelled</sub> were calculated as  $96.9 \pm 0.4\%$  and  $1.42 \pm 0.18$  (moles of dye per mole protein), respectively. In addition, Fig. 1 showed the excitation (maximum at 557 nm) and the emission (maximum at 582 nm) spectra of the  $\beta$ -CN<sub>labelled</sub> conjugate, while NHS-Rhodamine has an excitation maximum at 552 nm and emission maximum at 576 nm, which means that conjugation with  $\beta$ -CN caused a slight red-shift in both excitation and emission. Furthermore, SDS-PAGE analysis of  $\beta$ -CN and  $\beta$ -CN<sub>labelled</sub> showed that  $\beta$ -CN<sub>labelled</sub> migrated somewhat more slowly, which may be due to the slightly higher molecular weight of  $\beta$ -CN<sub>labelled</sub> compared to that of  $\beta$ -CN (Fig. 1 inset;  $M_w$  of NHS-Rhodamine is 528 Da).

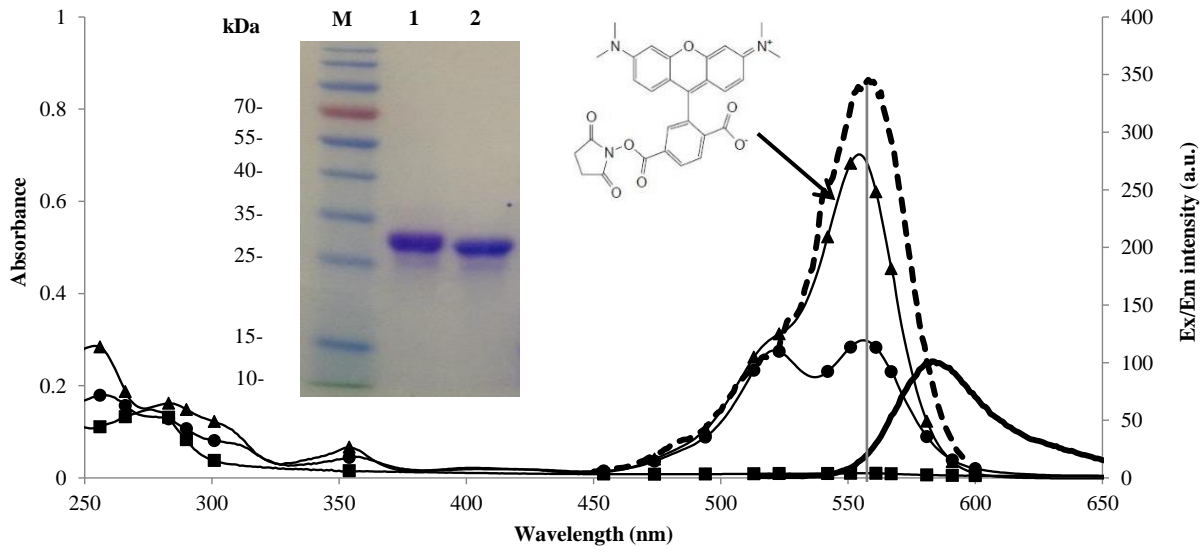


Fig. 1. Emission (solid line, excitation at 525 nm) and excitation (dashed line, emission at 600 nm) spectra of  $\beta$ -CN-Rhodamine conjugate ( $\beta$ -CN<sub>labelled</sub>) in 10 mM phosphate buffered saline, pH 7.4. Absorbance spectra of 5  $\mu$ g/ml NHS-Rhodamine (  $\blacktriangle$  ), 200  $\mu$ g/ml  $\beta$ -CN (  $\blacksquare$  ) and 120  $\mu$ g/ml  $\beta$ -CN<sub>labelled</sub> (  $\bullet$  ) were measured for comparison. The insets show the chemical structure of NHS-Rhodamine (right) and SDS-PAGE (left) of  $\beta$ -CN<sub>labelled</sub> (lane 1) and  $\beta$ -CN (lane 2); lane M represents molecular weight marker.

### 3.2 Effect of covalent labelling on the emulsification property of protein

The determination of interfacial tension between aqueous solutions and oil is useful for understanding the formation and stability of O/W emulsions. The type of aqueous solution affects the oil/aqueous interfacial tension. It should be noticed that the presence of small amounts of impurities (e.g. lecithin) in commercial sunflower oil can affect the interfacial tension of proteins. A decrease in the interfacial tension between the two phases increases the inherent thermodynamic stability of the emulsion (Gernon, Alford, Dowling, & Franco, 2009). Dynamic interfacial tension between solutions (e.g. sodium phosphate buffer pH 7.0, WPI,  $\beta$ -CN, WPI/ $\beta$ -CN or WPI/ $\beta$ -CN<sub>labelled</sub>) and sunflower oil over 60 min were recorded (Fig. 2). On formation of an interface between sunflower oil and phosphate buffer (used as a clean control interface), the initial interfacial tension ( $\gamma_i$ ) was  $18.7 \pm 1.3$  mN/m, then decreased to  $10.4 \pm 0.3$  mN/m once equilibrium interfacial tension ( $\gamma_{Eq}$ ) was reached after 60 min (Fig. 2); the decrease in interfacial tension

was generally achieved within 15 min of the interface formation. The measured  $\gamma_i$  and  $\gamma_{Eq}$  between oil and protein solutions were significantly lower than that of the clean interface, indicating the high effectiveness of proteins in reducing the interfacial tension. Compared with the oil/WPI system ( $\gamma_i = 11.9 \pm 0.2$  mN/m ,  $\gamma_{Eq} = 3.75 \pm 0.03$  mN/m), the interfacial tension of oil/ $\beta$ -CN significantly decreased from  $10.5 \pm 0.8$  to  $0.72 \pm 0.01$  mN/m. This means that  $\beta$ -CN is more surface-active than WPI in developing an oil/water interface. The effectiveness of  $\beta$ -CN in reducing the interfacial tension is due to its flexible and disordered secondary and tertiary structure (Dickinson, 1997; McClements, 2004). Results for the mixed protein systems were consistent with those of Seta, Baldino, Gabriele, Lupi, and Cindio (2014), who reported that the interfacial tension values for mixed whey protein/ $\beta$ -CN system fell between those of these proteins individually. The change in interfacial tension over time for the WPI/ $\beta$ -CN system was similar to that seen for  $\beta$ -CN alone (Fig. 2). When  $\beta$ -CN was replaced by  $\beta$ -CN<sub>labelled</sub> in WPI/ $\beta$ -CN system, there was no significant difference in  $\gamma_i$  and  $\gamma_{Eq}$  for both systems (Table 1), which shows that the labelling does not affect the emulsification property of  $\beta$ -CN.

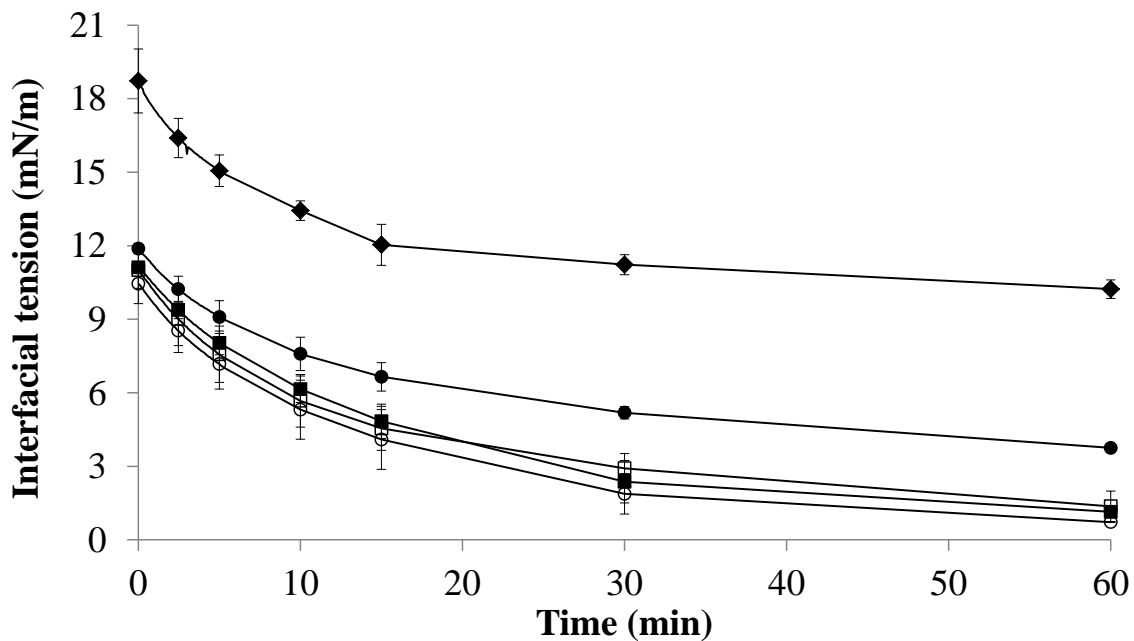


Fig. 2. Dynamic interfacial tension measured between sunflower oil and phosphate buffer (control) (♦), WPI alone (●),  $\beta$ -CN alone (○), a mixture of WPI/ $\beta$ -CN (1:1 by weight) (■) and a mixture of WPI/ $\beta$ -CN<sub>labelled</sub> (1:1 by weight) (□) at 20 °C, pH 7.0, using the Wilhelmy plate technique. Error bars represent the standard deviation of three independent replicates.

1 Table 1. Properties of O/W emulsions stabilized with WPI/ $\beta$ -CN or WPI/ $\beta$ -CN<sub>labelled</sub> at day 0 and 3 (mean  $\pm$  SD, n  $\geq$  3).

Emulsion type	Storage Day	Size D <sub>3,2</sub> ( $\mu$ m)	Size D <sub>4,3</sub> ( $\mu$ m)	$\zeta$ -potential	Viscosity (mPa.s) *	Creaming stability (%)	$\gamma_i$ (mN/m)	$\gamma_{Eq}$ (mN/m)
Emulsion-WPI/ $\beta$ -CN	0	1.65 $\pm$ 0.04 <sup>a</sup>	3.93 $\pm$ 0.18 <sup>a</sup>	-40.24 $\pm$ 2.17 <sup>a</sup>	3.91 $\pm$ 0.03 <sup>a</sup>	43.2 $\pm$ 1.4 <sup>a</sup>	11.1 $\pm$ 0.2 <sup>a</sup>	1.1 $\pm$ 0.1 <sup>a</sup>
Emulsion-WPI/ $\beta$ -CN	3	2.11 $\pm$ 0.24 <sup>b</sup>	5.61 $\pm$ 0.69 <sup>b</sup>	-	3.87 $\pm$ 0.00 <sup>a</sup>	-	-	-
Emulsion-WPI/ $\beta$ -CN <sub>labelled</sub>	0	1.63 $\pm$ 0.05 <sup>a</sup>	3.78 $\pm$ 0.27 <sup>a</sup>	-40.73 $\pm$ 2.11 <sup>a</sup>	3.85 $\pm$ 0.02 <sup>a</sup>	40.5 $\pm$ 1.4 <sup>a</sup>	11 $\pm$ 0.7 <sup>a</sup>	1.4 $\pm$ 0.1 <sup>a</sup>
Emulsion-WPI/ $\beta$ -CN <sub>labelled</sub>	3	1.61 $\pm$ 0.04 <sup>a</sup>	3.91 $\pm$ 0.39 <sup>a</sup>	-	3.82 $\pm$ 0.08 <sup>a</sup>	-	-	-

2

3 Within a column, values with different superscript letters are significantly different (p < 0.05).

4 \* Absolute viscosity at shear rate 300 s<sup>-1</sup> at 25 °C.

5 \*\* Integral light transmission value at 60 min at 25 °C.

### 6 3.3 Effect of covalent labelling on the physical behaviours of emulsions

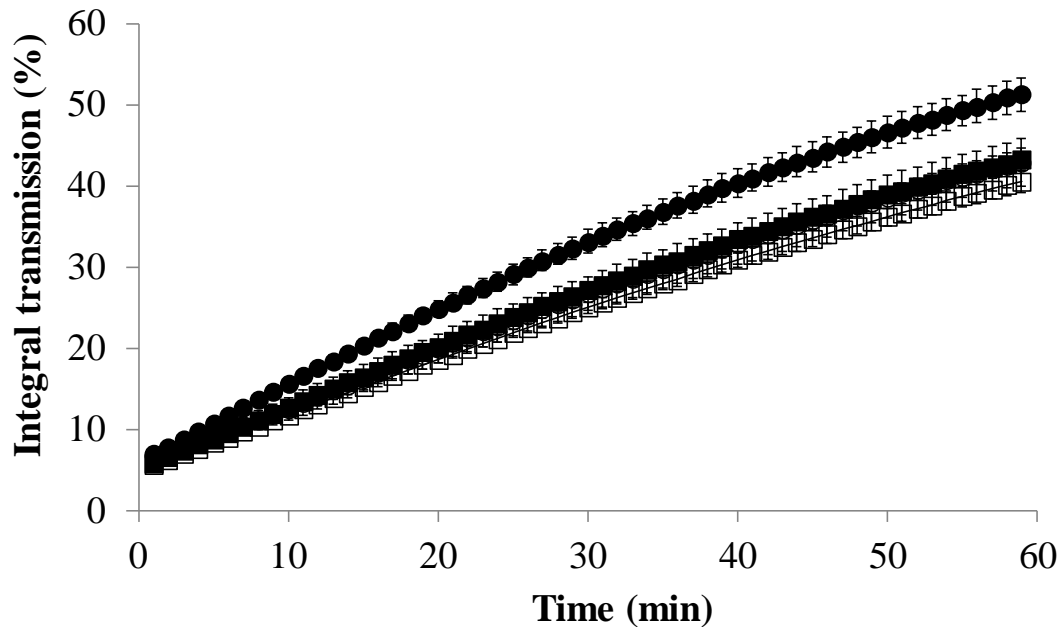
7 Fat droplet size of emulsions made with WPI/ $\beta$ -CN (control system) or WPI/ $\beta$ -CN<sub>labelled</sub> at day 0 and 3  
8 were measured (Table 1). The use of a lab homogenizer with low pressure (~ 4 MPa) resulted in  
9 emulsions with a droplet size distribution ranging from 0.28 – 111  $\mu$ m. No significant difference ( $p>0.05$ )  
10 in either  $D_{3,2}$  or the  $D_{4,3}$  was observed between fresh emulsions (day 0). After 3 days of storage at 4 °C,  
11 the droplet size of the control system markedly increased whereas the droplet size of the WPI/ $\beta$ -CN<sub>labelled</sub>  
12 emulsion did not change. Hence, according to the droplet size measurements, labelling of  $\beta$ -CN had no  
13 negative effect on fresh emulsions.

14

15 Fig. 3 shows the creaming stability of the four fresh emulsions, measured by a multiple analytical  
16 centrifuge (LUMiFuge). The slope of the integral transmission-time curve is an indicator of creaming  
17 stability, i.e. greater increases indicating lower stability. As shown in Fig. 3, the four emulsions had very  
18 similar integral transmission values (~ 6%) at the starting point. After 1 h centrifugation, the WPI-based  
19 emulsion presented the fastest increase in phase separation and the integral transmission (%) reached  $51.2$   
20  $\pm 2$ . Meanwhile, emulsions prepared with  $\beta$ -CN alone, a mixture of WPI/ $\beta$ -CN or a mixture of WPI/ $\beta$ -  
21 CN<sub>labelled</sub> had final values at  $42.8 \pm 2.9$ ,  $43.2 \pm 1.4$  and  $40.5 \pm 1.4$ , respectively. This confirms that  
22 emulsions made with WPI alone were the most unstable system compared to the other three emulsions.  
23 These results confirm previous observations by Parkinson, et al. (2004) that the addition of  $\beta$ -casein can  
24 inhibit the creaming effect of whey protein-based emulsions. From Fig. 3 it appears that emulsions  
25 stabilized with WPI/ $\beta$ -CN<sub>labelled</sub> were slightly more stable than those with WPI/ $\beta$ -CN. However, no  
26 significant difference ( $p>0.05$ ) in the creaming stability could be determined between them (Table 1).

27 The zeta ( $\zeta$ )-potential of WPI/ $\beta$ -CN- and WPI/ $\beta$ -CN<sub>labelled</sub>-based emulsions at pH 7.0 was also measured  
28 (Table 1). Both emulsions had negative apparent surface charges, around -40 mV, which indicates that  
29 covalent labelling technique did not significantly ( $p>0.05$ ) change the apparent surface charge of the  
30 emulsion droplets. Furthermore, all emulsions displayed Newtonian behaviour. The absolute viscosity of  
31 emulsions with or without label, at a shear rate of 300 s<sup>-1</sup> at day 0 and 3, are also shown in Table 1. After

32 three days storage at 4 °C, emulsions showed exactly the same behaviours throughout the shear rate range  
33 of 10-300 s<sup>-1</sup>; there was no significant difference (p>0.05) in viscosity at a shear rate of 300 s<sup>-1</sup> at 25 °C.

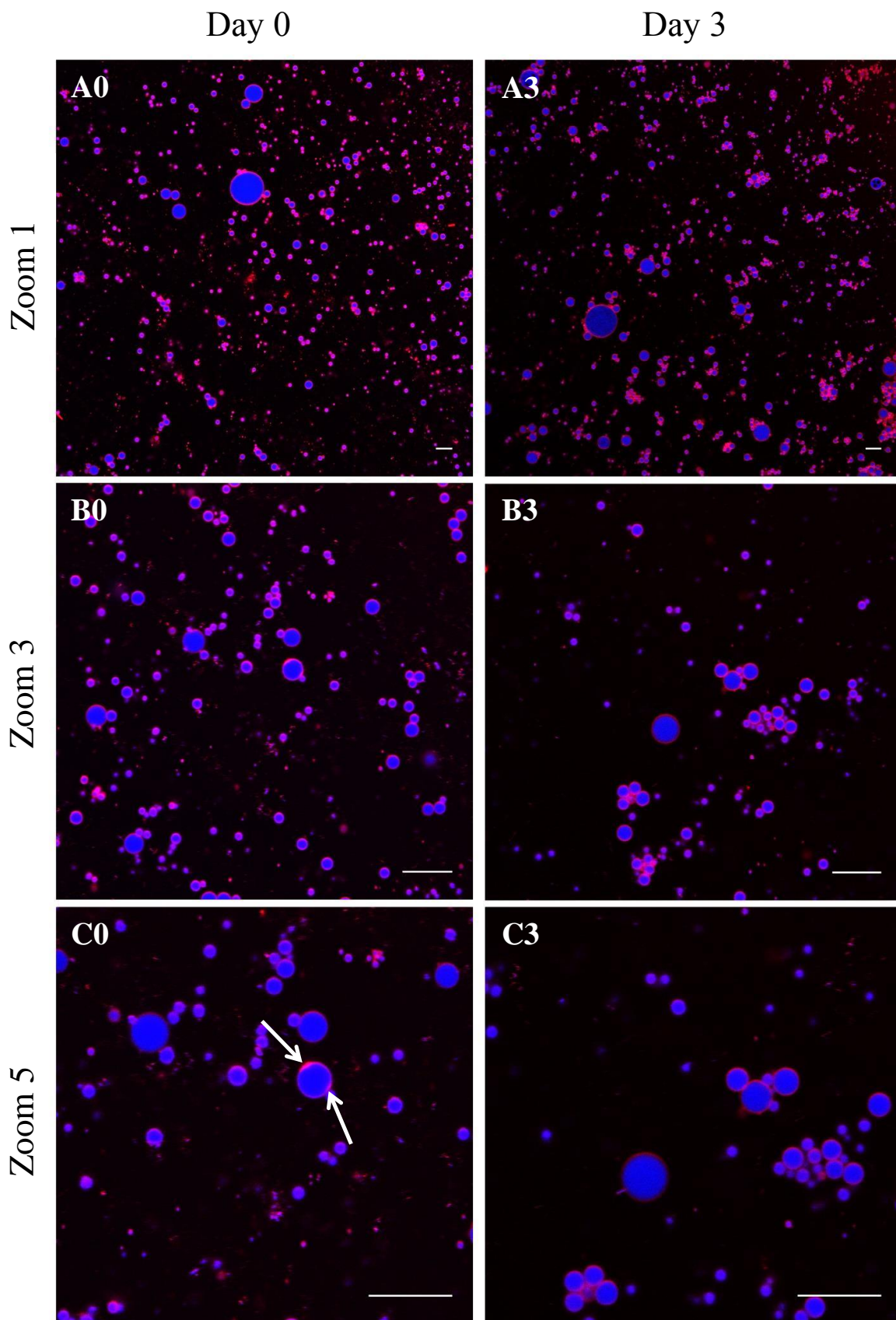


34  
35 Fig. 3. Creaming stability of fresh emulsions (10% sunflower oil, pH 7.0) made with a binary mixture of  
36 WPI/β-CN (1:1 by weight) (■), a mixture of WPI/β-CN<sub>labelled</sub> (1:1 by weight) (□), WPI alone (●) and β-  
37 CN alone (○), measured using a Lumifuge<sup>®</sup> stability analyser. Each data point is the average of four  
38 independent replicates.

#### 39 40 3.4 Microstructure of mixed protein-based emulsions

41 The CLSM images of WPI/β-CN-based emulsion (control system) at 0 and 3d are shown in Fig. 4. Both  
42 proteins and oil phase were non-covalently stained using Nile blue. It showed oil droplets  
43 (pseudocoloured blue) dispersed in a continuous phase generally with size less than 10 μm, which is  
44 consistent with the light scattering data (Table 1). Tromp, van de Velde, van Riel, and Paques (2001)  
45 stated the difficulty of testing functionality changes in covalently-labelled proteins due to the small  
46 quantities of labelled protein available. In this study, 0.5% (w/w) total protein was used as it was the  
47 minimum protein concentration required to prepare a stable emulsion. Proteins (pseudocoloured red)  
48 including WPI and β-CN were observed mostly at the surface of fat globules but not in the aqueous phase,  
49 which means there is no excess protein in this emulsion. In addition, it was found that the thickness of the

50 absorbed protein layers was variable and that these proteins may appear either as a monolayer or in dense  
51 aggregates (Fig. 4 image C0 and Fig. 5 image A4, arrows). Comparing the microstructure of emulsions  
52 during storage clearly showed that the oil droplets tend to flocculate after 3 d, presumably due to the low  
53 pressure used during homogenization resulting in an incomplete coverage of emulsifiers on the surface of  
54 oil droplets (McClements, 2004).



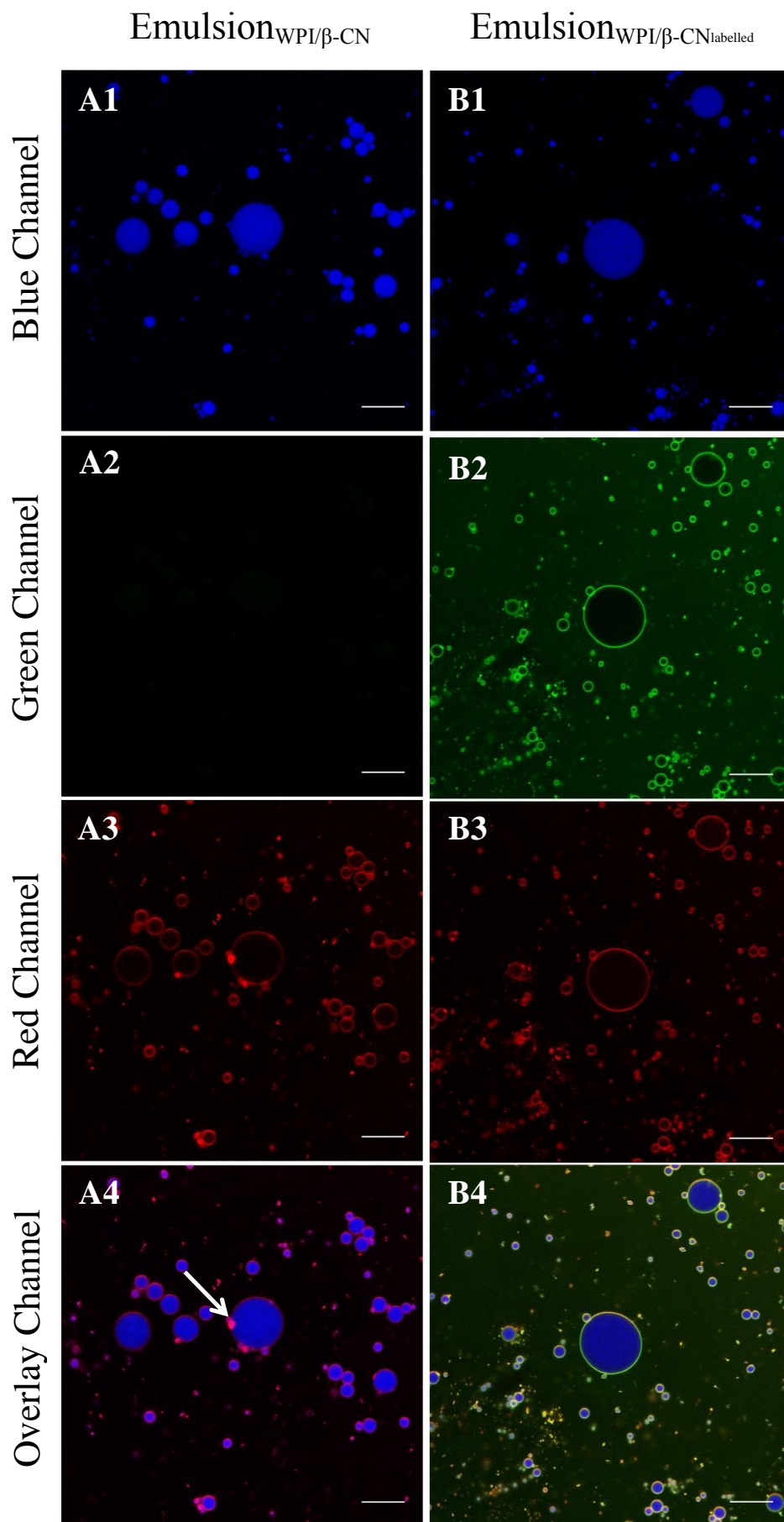
56 Fig. 4. Confocal micrographs of emulsions stabilized with WPI/ $\beta$ -CN acquired on day 0 (A0-C0) and 3  
57 (A3-C3) during storage at 4 °C, showing the fluorescence signal corresponding to the 488 and 633 nm  
58 laser excitation combined (Dual channel) at zoom 1, 3 and 5. Arrows indicate variable thickness of the  
59 protein layer at the oil droplet interface. Scale bar: 10  $\mu$ m.

60

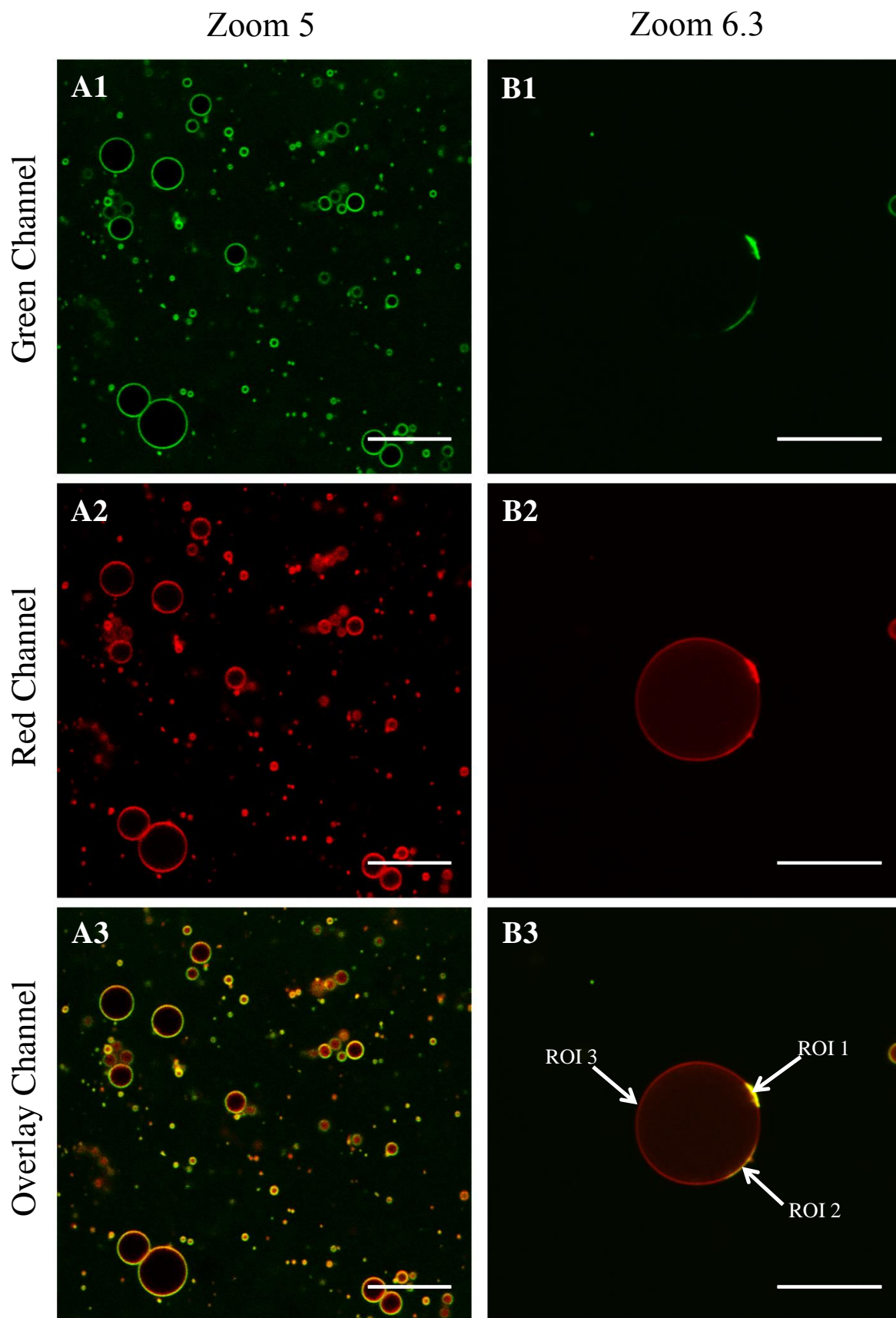
61 The nature of the adsorbed layer is one of the most important factors determining the stability of  
62 emulsions. A combination of covalent and non-covalent staining techniques was used to visualize two  
63 proteins on the interface. The CLSM micrographs of fresh emulsions made with mixed proteins (WPI/ $\beta$ -  
64 CN) and with covalently labelled mixed proteins (WPI/ $\beta$ -CN<sub>labelled</sub>) are shown in Fig. 5 (A1-A4, B1-B4).  
65 The images show fat globules pseudocoloured blue (image A1 and B1),  $\beta$ -CN pseudocoloured green  
66 (image B2), total proteins including both WPI and  $\beta$ -CN pseudocoloured red (image A3 and B3) and the  
67 overlay images (image A4 and B4), respectively.  $\beta$ -CN<sub>labelled</sub> could be observed in emulsions while non-  
68 covalently labelled  $\beta$ -CN could not be seen (image B2 and A2), indicating that the covalent labelling  
69 technique allowed visualization of  $\beta$ -CN in a mixed protein-stabilized emulsion and that the fluorescent  
70 probe was not affected by homogenization. Overlay images (Fig. 5 image B4 and Fig. 6 image A3 and  
71 B3), showed a mix of green and red pseudocolours on the O/W interface, indicating both whey proteins  
72 and  $\beta$ -CN were co-localized at the surface of fat globules. The adsorbed protein layer which is  
73 pseudocoloured either yellow (i.e. a mix of green and red channels) or green was  $\beta$ -CN, whilst WPI was  
74 pseudocoloured red. Therefore, WPI could be distinguished from  $\beta$ -CN in emulsions using covalent and  
75 non-covalent labels.

76 On increasing to higher zoom factors (Fig. 6), WPI (pseudocoloured red in the overlay channel, Fig. 6  
77 image A3) and  $\beta$ -CN (pseudocoloured yellow in the overlay channel, Fig. 6 image A3) were observed  
78 simultaneously and co-localized at the O/W interface. Images also revealed other information (Fig. 6  
79 image B1-B3), for example, pixel intensity of three regions of interest (ROI) labelled ROI 1, ROI 2 and  
80 ROI 3 taken at the interface was analysed using the Leica CLSM quantification tool. The pixel intensity  
81 of the green channel was the same as that of the red channel (~240) at ROI 1 while at ROI 2 the pixel  
82 intensity of red channel (106) was slightly higher than that of green channel (81). The intensity of green  
83 channel at ROI 3 was as low as that of the background (~13) whereas the red channel's intensity was 55,

84 which is much higher than its background (~6). All the free dye was expected to be removed by dialysis  
85 during the preparation of the  $\beta$ -CN-Rhodamine conjugate. Therefore, it was concluded that milk proteins  
86 were not evenly distributed at the surface of oil droplets and that the thickness of the interface depended  
87 on the type of protein. CLSM showed that  $\beta$ -CN produced a thicker layer (ROI 1 in Fig. 6 image B3) than  
88 whey proteins (ROI 3 in Fig. 6 image B3). This result appears to confirm the hypothesis of Parkinson and  
89 Dickinson (2004), who proposed that the absorbed whey protein layer was assumed to be thin, while the  
90 presence of casein molecules increased the effective thickness substantially, due to the “long dangling  
91 polypeptide tails” which are characteristic of  $\beta$ -CN molecules.



93 Fig. 5. Confocal micrographs of fresh emulsions stabilized with WPI/ $\beta$ -CN or WPI/ $\beta$ -CN<sub>labelled</sub> , showing  
94 the fluorescence signal corresponding to the 488 nm laser excitation (Blue channel, fat phase labelled by  
95 Nile Blue, image A1 and B1), the 561nm laser excitation (Green channel,  $\beta$ -CN labelled by Rhodamine,  
96 image A2 and B2), the 633 nm laser excitation (Red channel, all proteins labelled with Nile Blue, image  
97 A3 and B3) and the 488, 561 and 633 nm laser excitation combined (Overlay channel, image A4 and B4).  
98 The arrow indicates protein presented in dense aggregates on the surface of the oil droplet. Scale bar: 10  
99  $\mu$ m.



101 Fig. 6. Confocal micrographs of emulsions stabilized with WPI/ $\beta$ -CN<sub>labelled</sub> at different magnifications  
102 (zoom 5 and 6.3), showing the fluorescence signal corresponding to the 561 nm laser excitation (Green  
103 channel, image A1 and B1), the 633 nm laser excitation (Red channel, image A2 and B2) and the 561 and  
104 633 nm laser excitation combined (Overlay channel, image A3 and B3). Arrows indicate three regions  
105 (ROI 1, ROI 2 and ROI 3) of protein layer selected for image analysis. Scale bar: 10  $\mu$ m.

106

#### 107 4. Conclusion

108 This study has shown that the covalent labelling of  $\beta$ -CN with NHS-Rhodamine led to a minor effect on  
109 the spectral properties of NHS-Rhodamine. The emulsification properties of  $\beta$ -CN were not affected by  
110 conjugating with Rhodamine. The use of covalently labelled  $\beta$ -CN in a mixed casein/whey proteins  
111 emulsion demonstrated that the covalent labelling of  $\beta$ -CN also had no effect on the physicochemical  
112 properties of the emulsions. Combining covalent and non-covalent staining techniques with CLSM  
113 allowed localisation of two protein ingredients surrounding oil droplets in an O/W emulsion. Despite the  
114 resolution limits of the microscope ( $\sim$  250 nm), covalent labelling was shown to be a powerful approach  
115 that can be used to gain new insights in the surface properties of emulsions prepared with mixed proteins.

116

#### 117 5. Acknowledgements

118 The work was funded by the Irish Dairy Levy Research Trust. M. Li was funded under the Teagasc Walsh  
119 Fellowship Scheme. The authors would like to acknowledge K. Drapala from University College Cork,  
120 Cork, Ireland, for the help with measuring the interfacial tensions of protein solutions.

#### 121 6. References

- 122 Abhyankar, A. R., Mulvihill, D. M., Chaurin, V., & Auty, M. A. E. (2011). Techniques for localisation of  
123 konjac glucomannan in model milk protein-polysaccharide mixed systems: Physicochemical and  
124 microscopic investigations. *Food Chemistry*, 129(4), 1362-1368.
- 125 Auty, M. A. (2013). Confocal-microscopy: principles and applications to food microstructures. In V. J.  
126 M. Groves (Ed.), *Food Microstructures* (Vol. 4, pp. 96-98): Woodhead Publishing.
- 127 Auty, M. A., Twomey, M., Guinee, T. P., & Mulvihill, D. M. (2001). Development and application of  
128 confocal scanning laser microscopy methods for studying the distribution of fat and protein in  
129 selected dairy products. *Journal of Dairy Research*, 68(3), 417-427.
- 130 Brooker, B. E. (1995). Imaging food systems by confocal scanning laser microscopy. In E. Dickinson  
131 (Ed.), *New Physico-chemical Techniques for the Characterization of Complex Food Systems* (pp.  
132 53-68). London: Blackie Academic and Professional.
- 133 Ciron, C. I. E., Gee, V. L., Kelly, A. L., & Auty, M. A. E. (2010). Comparison of the effects of high-  
134 pressure microfluidization and conventional homogenization of milk on particle size, water

- 135 retention and texture of non-fat and low-fat yoghurts. *International Dairy Journal*, 20(5), 314-  
136 320.
- 137 Dauphas, S., Mouhous-Riou, N., Metro, B., Mackie, A. R., Wilde, P. J., Anton, M., & Riaublanc, A.  
138 (2005). The supramolecular organisation of  $\beta$ -casein: effect on interfacial properties. *Food*  
139 *Hydrocolloids*, 19(3), 387-393.
- 140 Dickinson, E. (1989). Surface and emulsifying properties of caseins. *Journal of Dairy Research*, 56(03),  
141 471-477.
- 142 Dickinson, E. (1997). Properties of Emulsions Stabilized with Milk Proteins: Overview of Some Recent  
143 Developments. *Journal of Dairy Science*, 80(10), 2607-2619.
- 144 Dickinson, E. (2001). Milk protein interfacial layers and the relationship to emulsion stability and  
145 rheology. *Colloids and Surfaces B: Biointerfaces*, 20(3), 197-210.
- 146 Dickinson, E., & Parkinson, E. L. (2004). Heat-induced aggregation of milk protein-stabilized emulsions:  
147 sensitivity to processing and composition. *International Dairy Journal*, 14(7), 635-645.
- 148 Dickinson, E., & Yamamoto, Y. (1996). Viscoelastic Properties of Heat-Set Whey Protein-Stabilized  
149 Emulsion Gels with Added Lecithin. *Journal of Food Science*, 61(4), 811-816.
- 150 Drapala, K. P., Auty, M. A. E., Mulvihill, D. M., & O'Mahony, J. A. (2015). Influence of lecithin on the  
151 processing stability of model whey protein hydrolysate-based infant formula emulsions.  
152 *International Journal of Dairy Technology*, 68(3), 322-333.
- 153 Fox, P. F., & McSweeney, P. L. H. (2003). *Advanced Dairy Chemistry: Volume 1: Proteins, Parts A&B*  
154 (3rd ed. Vol. 1). New York: Kluwer Academic/Plenum Publishers.
- 155 Gernon, M. D., Alford, D., Dowling, C. M., & Franco, G. P. (2009). Enhancing Oil/Water Emulsion  
156 Stability: The Use of Capillary Contact Angle Measurements to Determine Liquid/Liquid  
157 Interfacial Tensions between Aqueous Alkanolamine Solutions and Oils. *Tribology Transactions*,  
158 52(3), 405-414.
- 159 Guyomarc'h, F., Nono, M., Nicolai, T., & Durand, D. (2009). Heat-induced aggregation of whey proteins  
160 in the presence of  $\kappa$ -casein or sodium caseinate. *Food Hydrocolloids*, 23(4), 1103-1110.
- 161 Hammarsten, O. (1883). Zur Frage ob Casein ein einheitlicher Stoff sei. *Zeitschrift für Physiologische*  
162 *Chemie*, 7, 227-273.
- 163 Hunt, J. A., & Dalgleish, D. G. (1994). Adsorption behaviour of whey protein isolate and caseinate in  
164 soya oil-in-water emulsions. *Food Hydrocolloids*, 8(2), 175-187.
- 165 Kehoe, J. J., & Foegeding, E. A. (2011). Interaction between  $\beta$ -Casein and Whey Proteins As a Function  
166 of pH and Salt Concentration. *Journal of Agricultural and Food Chemistry*, 59(1), 349-355.
- 167 Kehoe, J. J., & Foegeding, E. A. (2014). The characteristics of heat-induced aggregates formed by  
168 mixtures of  $\beta$ -lactoglobulin and  $\beta$ -casein. *Food Hydrocolloids*, 39, 264-271.
- 169 L., L., Slyke, v., & Barker, J. C. (1918). The preparation of pure casein. *Journal of Biological Chemistry*,  
170 35, 127-136.
- 171 Laemmli, U. K. (1970). Cleavage of Structural Proteins during the Assembly of the Head of  
172 Bacteriophage T4. *Nature*, 227(5259), 680-685.
- 173 Lopez, C., Madec, M.-N., & Jimenez-Flores, R. (2010). Lipid rafts in the bovine milk fat globule  
174 membrane revealed by the lateral segregation of phospholipids and heterogeneous distribution of  
175 glycoproteins. *Food Chemistry*, 120(1), 22-33.
- 176 Maher, P. G., Auty, M. A. E., Roos, Y. H., Zychowski, L. M., & Fenelon, M. A. (2015). Microstructure  
177 and lactose crystallization properties in spray dried nanoemulsions. *Food Structure*, 3, 1-11.
- 178 McCarthy, N. A., Kelly, A. L., O'Mahony, J. A., & Fenelon, M. A. (2013). The physical characteristics  
179 and emulsification properties of partially dephosphorylated bovine  $\beta$ -casein. *Food Chemistry*,  
180 138(2-3), 1304-1311.
- 181 McClements, D. J. (2004). Protein-stabilized emulsions. *Current Opinion in Colloid & Interface Science*,  
182 9(5), 305-313.
- 183 McSweeney, S. L., Mulvihill, D. M., & O'Callaghan, D. M. (2004). The influence of pH on the heat-  
184 induced aggregation of model milk protein ingredient systems and model infant formula  
185 emulsions stabilized by milk protein ingredients. *Food Hydrocolloids*, 18(1), 109-125.
- 186 Millqvist-Fureby, A., Elofsson, U., & Bergenstahl, B. (2001). Surface composition of spray-dried milk  
187 protein-stabilised emulsions in relation to pre-heat treatment of proteins. *Colloids and Surfaces B:*  
188 *Biointerfaces*, 21(1-3), 47-58.

- 189 Mitchell, J., Irons, L., & Palmer, G. J. (1970). A study of the spread and adsorbed films of milk proteins.  
190 *Biochimica et Biophysica Acta (BBA) - Protein Structure*, 200(1), 138-150.
- 191 Morgan, P. E., Treweek, T. M., Lindner, R. A., Price, W. E., & Carver, J. A. (2005). Casein Proteins as  
192 Molecular Chaperones. *Journal of Agricultural and Food Chemistry*, 53(7), 2670-2683.
- 193 O’Kennedy, B. T., Mounsey, J. S., Murphy, F., Duggan, E., & Kelly, P. M. (2006). Factors affecting the  
194 acid gelation of sodium caseinate. *International Dairy Journal*, 16(10), 1132-1141.
- 195 Parkinson, E. L., & Dickinson, E. (2004). Inhibition of heat-induced aggregation of a  $\beta$ -lactoglobulin-  
196 stabilized emulsion by very small additions of casein. *Colloids and Surfaces B: Biointerfaces*,  
197 39(1–2), 23-30.
- 198 Raikos, V. (2010). Effect of heat treatment on milk protein functionality at emulsion interfaces. A review.  
199 *Food Hydrocolloids*, 24(4), 259-265.
- 200 Rollema, H. S. (1992). Casein association and micelle formation. In P. F. FOX (Ed.), *Advanced Dairy*  
201 *Chemistry: Proteins* (Vol. 1, pp. 111-141). London: Elsevier Science Publishers.
- 202 Seta, L., Baldino, N., Gabriele, D., Lupi, F. R., & Cindio, B. d. (2014). Rheology and adsorption  
203 behaviour of  $\beta$ -casein and  $\beta$ -lactoglobulin mixed layers at the sunflower oil/water interface.  
204 *Colloids and Surfaces A: Physicochemical and Engineering Aspects*, 441, 669-677.
- 205 Tromp, R. H., van de Velde, F., van Riel, J., & Paques, M. (2001). Confocal scanning light microscopy  
206 (CSLM) on mixtures of gelatine and polysaccharides. *Food Research International*, 34(10), 931-  
207 938.
- 208 van de Velde, F., Weinbreck, F., Edelman, M. W., van der Linden, E., & Tromp, R. H. (2003).  
209 Visualisation of biopolymer mixtures using confocal scanning laser microscopy (CSLM) and  
210 covalent labelling techniques. *Colloids and Surfaces B: Biointerfaces*, 31(1–4), 159-168.  
211

